

Curvature Induced *L*-Defects in Water Conduction in Carbon Nanotubes

Urs Zimmerli, Pedro G. Gonnet, Jens H. Walther, and Petros Koumoutsakos*

Institute of Computational Science, ETH Zürich, Switzerland

Received February 18, 2005; Revised Manuscript Received April 15, 2005

ABSTRACT

We conduct molecular dynamics simulations to study the effect of the curvature induced static dipole moment of small open-ended single-walled carbon nanotubes (CNTs) immersed in water. This dipole moment generates a nonuniform electric field, changing the energy landscape in the CNT and altering the water conduction process. The CNT remains practically filled with water at all times, whereas intermittent filling is observed when the dipole term is not included. In addition, the dipole moment induces a preferential orientation of the water molecules near the end regions of the nanotube, which in turn causes a reorientation of the water chain in the middle of the nanotube. The most prominent feature of this reorientation is an *L*-defect in the chain of water molecules inside the CNT. The analysis of the water energetics and structural characteristics inside and in the vicinity of the CNT helps to identify the role of the dipole moment and to suggest possible mechanisms for controlled water and proton transport at the nanoscale.

Introduction. Nanoscale molecular sieves are ubiquitous in biological systems, and biological pores transporting water are essential for living organisms ranging from bacteria to animals and plants.¹ The low reactivity of carbon nanotubes (CNTs) with a number of substances and their structural stability has prompted a number of investigations on their suitability as artificial nanopores and ion channels. Biological channels, however, show quite a heterogeneous interior that is largely responsible for their specific biological functions.² For example, two extensively studied biological pores, gramicidin and aquaporin, both contain single file water structures, but they differ in their permeability for proton transport. Proton transport occurs rapidly through gramicidin but it is inhibited for aquaporins.^{3,4} These differences in proton permeability are attributed to the chemical structure of the pore itself. This chemical structure in turn determines the electrical field inside the pore, influencing the structure of the single-file water chain.⁴

The influence of pore charge groups and dipole moments in biological systems are responsible for the preferential transport and orientation of the water molecules.^{4,5} In CNTs, inhomogeneities on their interior are often associated with the presence of impurities induced during fabrication. However, in recent *ab initio* calculations, Dumitrica et al.⁶ found a significant static dipole moment across CNT walls that is not present in graphitic systems. This static dipole moment per carbon atom is inversely proportional to the curvature radius of the CNT and is oriented radially toward the tube axis. The presence of the curvature induced dipole moment induces an electric field in the interior of the

nanotube that alters its interaction with charged and polar molecules. This interaction has important ramifications for the transport of water molecules inside CNTs, in particular if small tube diameters and short lengths are considered.

Understanding the interaction of water with CNTs is essential for the rational design of nanopores for water transport and has been subject to intense research efforts.^{8–13} Despite the hydrophobic nature of CNTs,⁸ Hummer et al. first demonstrated that a short CNT could fill with a single line of water molecules and could therefore act as a possible model system for biological channels.¹¹ Note that single-file water chains appear in several biological pores that have a constriction, such as gramicidin and aquaporin, but this is not generally the case.

A number of studies have been conducted to quantify the influence of different system properties such as the pore diameter, the tube helicity,¹⁴ and the strength of the water carbon interaction.¹⁵ More recent studies have focused on the mechanics of filling and the ordering of water molecules inside the CNT. Mann and Halls¹⁶ studied proton transport through a CNT, and Dellago et al.¹⁷ showed that defects within the quasi one-dimensional hydrogen bonded chain of water molecules could significantly alter the rate of proton transport through a CNT. Zhu and Schulten⁵ quantified this effect using a statistical analysis and considered the influence of charged atoms in the tube wall equivalent to having dipole moments parallel to the tube axis.

The potentials used in all MD simulations involving carbon nanotubes, to the best of our knowledge, are inferred from graphitic systems and do not consider effects induced by CNT-intrinsic properties such as curvature.⁷ The interaction

* Corresponding author. E-mail: petros@inf.ethz.ch.

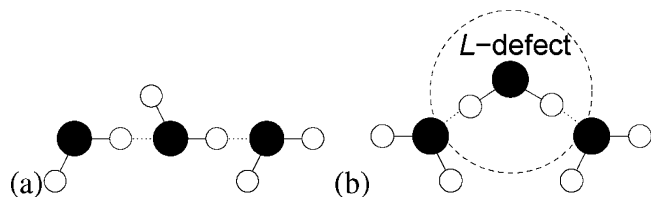


Figure 1. In (a) a quasi-one-dimensional hydrogen bonded chain of water molecules is depicted where each water molecule acts as a hydrogen bond donor to one of its neighbors and as an acceptor to the other. In (b) the central water molecule acts as a hydrogen bond donor to both of its neighbors and thus forms an *L*-defect. The hydrogen bonds are indicated with dotted lines. The water molecules are represented by a set of three circles, where the filled ones indicate oxygen and the unfilled indicate hydrogen atoms.

of CNTs and water is modeled by a Lennard-Jones interaction between the water oxygen atoms and carbon atoms (see ref 18 and references therein). Electrostatic interactions between the water atoms and the CNT have been taken into account in a few studies as charge-induced dipole interaction¹⁹ and charge-quadrupole interactions.^{19,8}

In this work we model the CNT curvature-induced dipole moment following the work of Dumitriča et al.,⁶ and we report on the results of MD simulations of finite-length single-walled CNTs (SWCNTs) immersed in water. The simulations show an increased filling and a geometrical rearrangement of the single-file water chain inside the tube. The water molecules are strongly affected by the curvature-induced dipole of the CNT, and they get reoriented inside the CNT so that a water molecule within the chain acts as a hydrogen bond donor to both its neighbors, resulting in an *L*-defect,¹⁷ see Figure 1. This *L*-defect may interfere with the ability of CNTs to transport protons, as fast proton transfer according to the Grotthuss mechanism becomes impossible.¹⁷ The analysis of the water energetics and structural characteristics inside and in the vicinity of the CNT help to identify the role of the dipole moment and to suggest possible mechanisms for controlled water and proton transport at the nanoscale.

Methodology. We perform MD simulations of a short CNT in armchair configuration with a chiral vector of (6,6), corresponding to a tube diameter of 0.81 nm. The tube is 1.34 nm long, corresponding to the CNT originally studied in ref 11. The present model employs the SPC/E²¹ water model and describes the nonpolar interaction between water and carbon using a Lennard-Jones potential between the carbon and oxygen atoms. We use the interaction parameters proposed by Werder et al.¹⁸ with $\epsilon_{CO} = 0.392 \text{ kJ mol}^{-1}$ and $\sigma_{CO} = 0.319 \text{ nm}$, which were found to reproduce the experimental contact angle of water on a graphite surface of 86° . All Lennard-Jones interactions are truncated at a cutoff distance of 1 nm, whereas the electrostatic interactions are calculated using the smooth particle mesh Ewald (SPME) method.²² The parameter determining the decay of the real part of the interaction potential for the SPME method is set to 3.0 nm^{-1} , and the charges are interpolated using fourth order B-splines to a mesh with $80 \times 48 \times 16$ grid points. Given the size of the computational box of 13.614×9.498

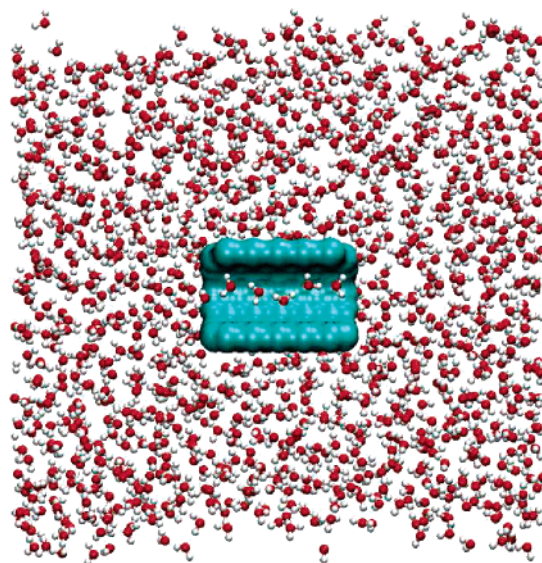


Figure 2. Cross-section of the simulation setup showing the CNT in a slab of 2464 water molecules. The tube is oriented parallel to the slab of water and its free surfaces.

$\times 3.166 \text{ nm}$, this results in a maximal grid spacing of less than 0.2 nm.

The curvature-induced static dipole moment per carbon atom is calculated according to the relationship proposed by Dumitriča et al.⁶ For a CNT with a diameter of 0.8 nm the dipole moment is 0.2 D per carbon atom. We model the static dipole moment across the CNT surface by placing two particles with charges of 0.5e and $-0.5e$ displaced by $4.16 \times 10^{-3} \text{ nm}$ radially inside and outside the CNT from each carbon atom. This approach allows for the treatment of all electrostatic interactions within the standard SPME method. The relative error between the interaction energy of a point dipole interacting with a charge at distances larger than 0.2 nm and the current model is smaller than 0.05%, that is less than the uncertainty of the underlying model.⁶

The CNT is placed in the center of the computational box and 2464 water molecules are placed in a slab configuration around the CNT with the free surfaces parallel to the tube axis, see Figure 2. Atmospheric conditions are ensured throughout the simulations by the free surfaces of the water slab. This approach avoids possible artifacts introduced by a barostat through the calculation of pressure and the large empty volume in the interior of the CNT. The orientation and the position of the tube are kept rigid and fixed in the center of the computational box throughout the simulation. The center of mass of water is constrained in order to prevent the water slab from expelling the essentially hydrophobic CNT after long simulation times. The system is equilibrated for 0.2 ns at a temperature of 300 K using a Berendsen thermostat with a coupling constant of 0.1 ps. After equilibration, the thermostat is turned off and the simulations are run in the microcanonical ensemble for approximately 12 ns with samples collected every 0.2 ps.

Two setups are considered to assess the effect of the static dipole moment: (i) Case P: A 1.35 nm SWCNT immersed in a slab of water without modeling of the dipole moment;

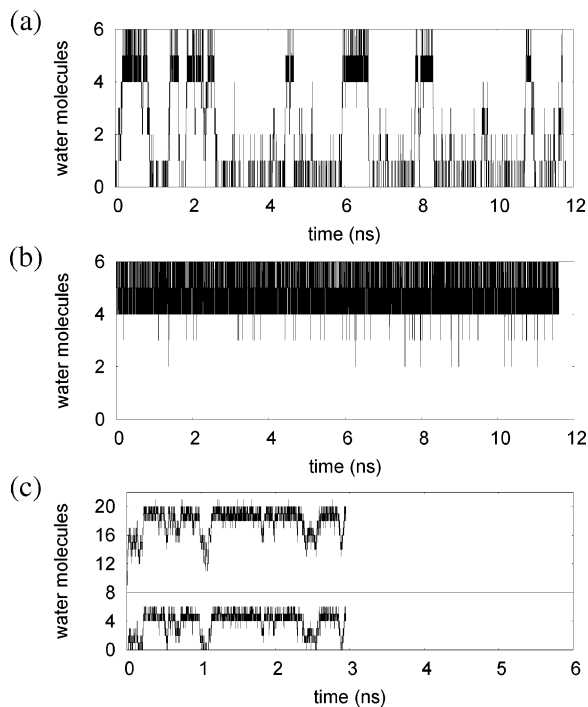


Figure 3. Panels (a) and (b) show the time history of the number of water molecules inside a 1.35 nm CNT as a function of simulation time. In (a) the CNT is modeled without and in (b) with a static dipole moment. Panel (c) shows the number of water molecules in a 2.7 nm CNT with a dipole moment in the top part and below the number of water molecules in the central 50% of the same tube. The coinciding emptying events in both plots show that the breaking of the water chain occurs in the center of the tube and not at the ends.

(ii) Case D: A 1.35 nm SWCNT with a static dipole moment modeled as described in the previous section. All other parameters of the setup are the same as those of Case P. Furthermore, we consider simulations of CNTs with lengths of 1.5 and 2.7 nm to study the influence of the length on the filling of the CNT.

Results and Discussion. In case P we validate our setup by monitoring water conduction in a SWCNT immersed in water, following the original work of Hummer et al.¹¹ Figure 3a shows the evolution of the number of water molecules inside the CNT during the course of the simulation. The water occupancy of the CNT fluctuates with sharp transitions between two distinct states of an empty and a filled nanotube throughout the simulation, consistent with results reported by Hummer et al.¹¹ However, in this study the CNT was filled 11% of the time, while we observe for our setup a filled state in 25% of the 12 ns simulation. This increased filling is attributed to the energy of the water–carbon Lennard-Jones interaction potential¹⁸ used in the present study, that is 45% stronger than the one used in the reference work of Hummer et al.¹¹ The filling of the CNT is found to be very sensitive to the interaction potential, and an increase of 10% for the present carbon–oxygen Lennard-Jones interaction energy results in a permanent filling with occupancy graphs similar to those shown in Figure 3b. This result is consistent with results reported by Hummer et al.¹¹ and Waghe et al.¹⁵ During the course of the simulation, 66

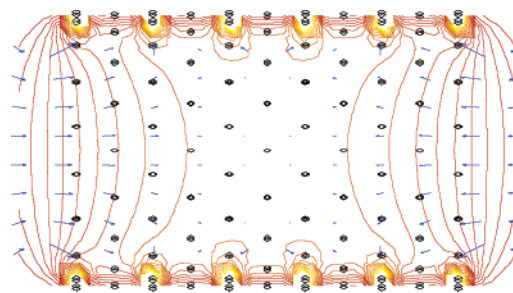


Figure 4. The electric field due to the static dipole moment across the nanotube wall is strongest 0.004 nm outside the tube entrances, pointing into the carbon nanotube along the axis of the CNT. Toward the middle of the tube, the axial components of the electric field vanish. In this figure, the positions of the carbon atoms are indicated by black dots, the field direction and magnitude by arrows and the field force by red isolines.

water molecules were found to enter the CNT from one side and leave on the other. The transport of water molecules through the tube amounts to approximately 22 molecules per nanosecond while the tube is filled. This number is within the range of transport rates reported by Hummer et al.,¹¹ who observed an average of 17 molecules per nanosecond and variations between 9 and 30 molecules per nanosecond. Water molecule flow rates and occupancy of the CNT are in quantitative agreement with the results reported in refs 11 and 15, and there is similar qualitative behavior regarding the emptying and filling of the nanotube.

In case D, the effect of the curvature induced dipole moment on the filling and water conduction through the CNT is studied using all other parameters as in case P. The simulations show that water molecules fill the CNT immediately and that it remains filled for the course of the entire simulation, cf. Figure 3b, with very short intervals of lower occupancy. The rate of transport of water molecules through the CNT amounts to 10 molecules per nanosecond. This rate of transport is lower than the corresponding rate for a tube without a dipole moment. We attribute the strong preference for the filled state in this case to an increased interaction of the water molecules with the electric field generated by the dipole moment distributed across the short nanotube, cf. Figure 4. The field is strongest toward the tube entrances with the leading components in the axial direction, pointing into the tube. Toward the center of the tube the axial components vanish and the electric field is radially oriented.

The dipole moment affects the orientation of the water molecules inside the CNT and the orientation of the water dipole moment relative to the tube axis. The radial density profiles for oxygen and hydrogen atoms inside the CNT, cf. Figure 5, exhibit small differences between case P and case D: the hydrogen density is slightly shifted toward the center of the tube and the oxygen density is slightly shifted toward the tube wall. However, the orientation of the water dipole moment differs significantly, cf. Figure 6 between the two cases. In case P a unidirectional hydrogen bonded chain is formed, similar to the one reported in refs 11 and 23, with a high probability of the orientation of the water dipole moment to form angles of 30° and 150° with the tube axis. The oxygen–carbon interaction acts so as to confine the

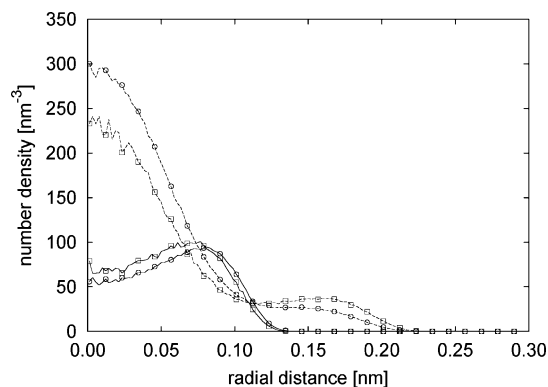


Figure 5. Radial number density distributions [nm^{-3}] within the tube are shown for oxygen (solid lines) and hydrogen atoms (dashed lines) for a CNT without (squares) and with (circles) a static dipole moment. The radial number density distribution of oxygen atoms shows a maximum around 0.09 nm, whereas the distribution for hydrogen has a clear maximum at the tube center with a shoulder toward larger radii.

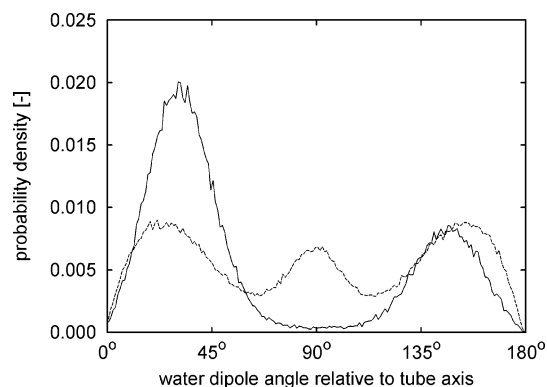


Figure 6. Probability density distribution of the angle between the water dipole moment and the tube axis. The asymmetric shape in the case without a dipole moment (solid line) is due to the limited sample size. For an angle of 0° (180°) the water dipole is parallel (antiparallel) to the tube axis, for an angle 90° it is perpendicular to the tube axis. An additional peak in probability around 90° is observed for the CNT with a static dipole moment (dashed line). This peak is attributed to the presence of an *L*-defect.

water oxygens to a cylinder with radius of 0.1 nm, cf. Figure 5, while the orientation of the water dipole is determined by the hydrogen bonding in the water chain inside the nanotube (Figure 7a). In case D the presence of the electric field triggers an orientational change within the chain of water molecules. The peaks of the original probability distribution (Figure 6) are shifted to 25° and 155° . Additionally, there is a peak around 90° that is associated with the presence of an *L*-defect.¹⁷ *L*-defects appear when a water molecule in the hydrogen bonded chain acts as a hydrogen bond donor to both of its two neighboring water molecules. This is confirmed by observations of water molecules inside the CNT, cf. Figure 7b, showing the existence of an *L*-defect. This defect has significant influence on the proton transport rates in quasi one-dimensional water chains.^{17,5} The angle of the water dipole moment changes across such a defect from approximately 30° on one side of the *L*-defect to about 90° at the defect and approximately 150° on its other side (cf. Figures 6 and 7b). The shift in the probability distribution

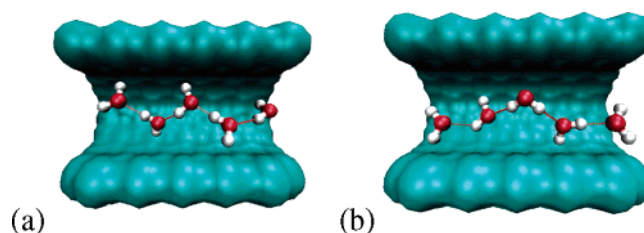


Figure 7. Typical water organization inside (a) a CNT without and (b) a CNT with a static dipole moment. In the CNT without a dipole moment the water molecules form a uniformly oriented hydrogen bond chain. In the CNT with a static dipole moment the directionality is opposite toward either end and in the middle a water molecule donates two hydrogen bonds and accepts none, i.e., it forms an *L*-defect.

between case P and case D is mainly due to a reorientation of the water molecules near the entrance of the nanotube, while the peak at 90° is due to the presence of the *L*-defect at the center of the tube. The formation of an *L*-defect is energetically unfavorable when considered on its own. More specifically, the difference in the interaction energy between three water molecules in a single hydrogen bonded chain and three water molecules forming an *L*-defect is found to be on average 8 kJ mol^{-1} . However, favorable overall energetics are obtained when the interactions of the CNT dipole moment with the water molecules near the entrance of the CNT are also considered. Even only a single water molecule in the electric field at the entrance of the tube experiences a reduction in potential energy of about 16 kJ mol^{-1} , with respect to case P, if its dipole is pointing away from the tube.

At the entrance, the CNT dipole moment reaches its maximum strength (3.5 V nm^{-1}) and it affects strongly the nearby water molecules, orienting them along the axis of the CNT while pointing to the opposite direction of the electric field. The interaction of the reoriented water molecules with the electric field is the main contributor to the change in interaction energy leading to the strong preference of the filled state (Figure 3) and the presence of the *L*-defect at the middle of the nanotube. This finding is consistent with the results from a recent study by Vaitheeswaran et al.²³ In their work it was shown that for a constant external electric field of 1 V nm^{-1} a filled CNT is energetically more favorable than an empty one, with the water dipoles collectively oriented against the direction of the electric field. The electric field induced by the nanotube dipole results in a reorientation of the water molecules, similar to the effect of an external electric field, albeit in opposite directions at each entrance. Hence, two chains of water dipoles with opposite orientations are favorable in either half of the nanotube. In the center of the tube the electric field is weakest with its leading components in the radial direction. This favors the alignment of a water molecule with its dipole normal to the tube axis. With a water molecule in this orientation in the middle of the tube, two hydrogen bonded chains with opposite orientation can be accommodated in either half of the nanotube. Hence, the resulting *L*-defect in the center of the nanotube accommodates the energetically favorable water orientations at each end of the tube.

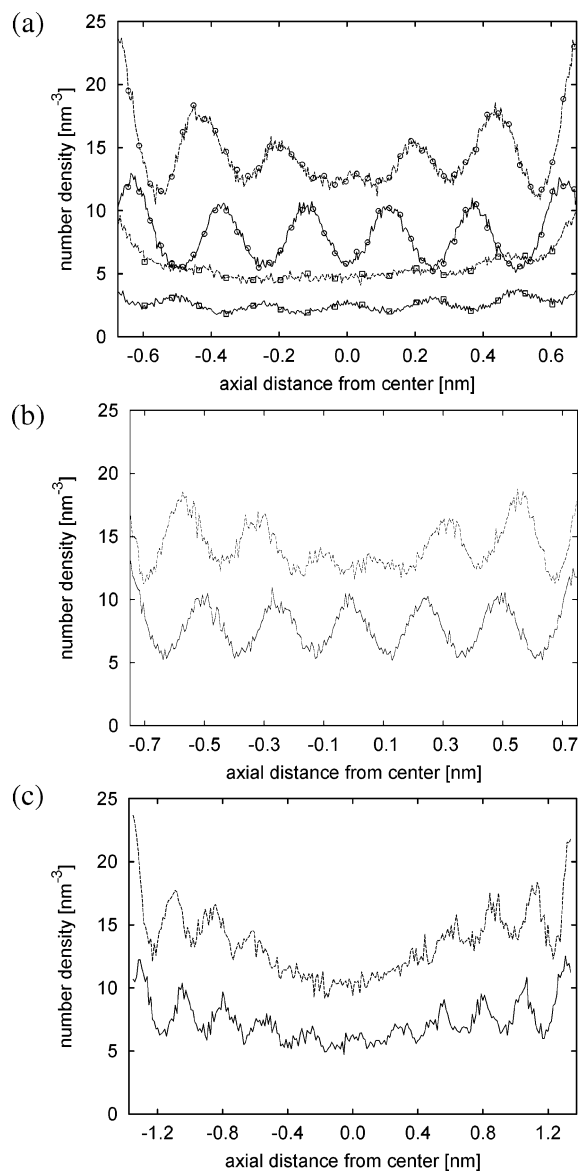


Figure 8. (a) Oxygen (solid lines) and hydrogen (dashed lines) number densities are shown inside a CNT along the tube axis for a CNT of 1.35 nm length. The CNT is modeled without a dipole moment (squares) and with a dipole moment (circles), respectively. The oxygen density profile shows six peaks in the presence of a dipole compared to five in its absence. For the tube with a dipole, the hydrogen density peaks are staggered with regard to the oxygen density peaks. The lack of a peak in hydrogen density at the center of the tube indicates the presence of an *L*-defect. The number densities in (b) and (c) are for a CNT with a dipole moment of 1.5 and 2.7 nm length, respectively. The results for the 1.5 nm tube are similar to the results obtained for the 1.35 nm tube. For the 2.7 nm tube, distinct maxima in the oxygen density are present toward the tube ends and become less pronounced toward the center of the tube. Toward the center of the tube the local density maxima for hydrogen disappear for the 1.5 nm CNT.

The axial number density profiles of the oxygen and hydrogen atoms shown in Figure 8a indicate increased structuring of the water molecules inside the tube for case D as compared to case P. This increase in structure is attributed to a change in sign of the gradient of the electric field at the tube entrances, cf. Figure 4. Outside this region, water molecules with their dipole moment pointing away

from the tube are pulled toward the tube. Inside the tube, water molecules with their dipole moment pointing out of the tube are pushed toward the end. This results in an effective compression of the water molecules at the entrance region of the tube, that results in the aforementioned structuring. This structuring is more pronounced for shorter nanotube lengths. The 1.35 nm tube accommodates an even number of six water molecules inside the tube, cf. Figure 8a. Thus, on average there are two water molecules around the tube center that are equally likely to participate in an *L*-defect, with the location of the *L*-defect switching dynamically between the two. This is demonstrated by the axial number density profile for the oxygen atoms, that does not show a density peak at the tube center, cf. Figure 8a. The hydrogen density profile lacks a peak between the two off-center oxygen density peaks. A slightly longer tube (1.5 nm) with the same dipole moment fits an additional molecule, containing a total of seven water molecules, cf. Figure 8b. This results in a density peak for oxygen atoms in the center of the tube while symmetrically around it two hydrogen density peaks indicate the position of the *L*-defect. For short nanotubes the axial components of the electric field directly determine the water structure throughout the tube. This is reflected by an augmented structure within the oxygen density, which is found to persist throughout the 1.35 nm CNT. The oxygen density structure in the 1.5 nm CNTs is not significantly different although a relative reduction of structuring is observed. However, for nanotubes longer than 2 nm the axial components of the electric field affect the water structure only near the entrance of the nanotube. Thus the peaks in the oxygen density profile for the 2.7 nm long carbon nanotube persists near the tube ends while in the center of the tube the density peaks become less expressed, cf. Figure 8b and Figure 8c. In addition, while this longer CNT most of the time exhibits full occupancy, we also observe intervals where about half of the water molecules leave the tube, cf. Figure 3c. The partial emptying is primarily affecting the occupancy in the middle of the tube as observed by comparing the occupancy of the whole tube with the occupancy of the central 50%, cf. Figure 3c. This reduction in occupancy, for the increased length of the nanotube, is consistent with the reduction in strength of the axial component of the electric field at the center of the nanotube.

Concluding Remarks. We have studied the effect of the curvature-induced static dipole moment on water conduction in short SWCNTs. This dipole moment induces an inhomogeneity in the characteristics of the CNT giving rise to an axial electric field that is strongest at the tube entrances and smaller toward the middle of the tube. This field has a significant influence on both the filling behavior and the orientation of water molecule chains inside the CNT as well as at its entrance. In particular, the presence of the dipole moment gives rise to an *L*-defect in the quasi one-dimensional water chain inside the tube. This effect could have major implications in the use of CNTs as nanoscale pores or channels.^{5,17} Specifically, controlled proton conduction could be achieved by suitably manipulating an external

electric field superimposed on the electric field of the CNT curvature-induced dipole.

Moving toward realistic nanopore systems, we need to consider CNT arrays embedded in membranes and to compare water transport in this case with corresponding simulations of transport across biological pores embedded in membranes.^{24,25} Such simulations need to take into account the curvature-induced dipole of the CNT as discussed in this work and its interplay with the considerable surface electric field of the membranes.

Acknowledgment. We thank Boris I. Yakobson from Rice University for the motivation to pursue these studies. We thank Richard Jaffe (NASA Ames) and Michele Parrinello (ETHZ) for several fruitful discussions.

References

- (1) Preston, G. M.; Carroll, T. P.; Guggino, W. B.; Agre, P. *Science* **1992**, *256*, 385–387.
- (2) Grubmüller, H. *Proc. Natl. Acad. Sci. U.S.A.* **2003**, *100*(13), 7421–7422.
- (3) Pomès, R.; Roux, B. *Biophys. J.* **2002**, *82*, 2304–2316.
- (4) Tajkhorshid, E.; Nollert, P.; Jensen, M. Ø.; Miercke, L. J. W.; O’Connell, J.; Stroud, R. M.; Schulten, K. *Science* **2002**, *296*, 525–530.
- (5) Zhu, F.; Schulten, K. *Biophys. J.* **2003**, *85*(1), 236–244.
- (6) Dumitriča, T.; Landis, C. M.; Yakobson, B. I. *Chem. Phys. Lett.* **2002**, *360*(1–2), 182–188.
- (7) Koumoutsakos, P. *Annu. Rev. Fluid Mech.* **2005**, *37*, 457–487.
- (8) Walther, J. H.; Jaffe, R.; Halicioglu, T.; Koumoutsakos, P. *J. Phys. Chem. B* **2001**, *105*, 9980–9987.
- (9) Werder, T.; Walther, J. H.; Jaffe, R.; Halicioglu, T.; Noca, F.; Koumoutsakos, P. *Nano Lett.* **2001**, *1*(12), 697–702.
- (10) Gordillo, M. C.; Martí, J. *Phys. Rev. B* **2003**, *67*, 205425-1–205425-4.
- (11) Hummer, G.; Rasaiah, J. C.; Noworyta, J. P. *Nature* **2001**, *414*, 188–190.
- (12) Beckstein, O.; Sansom, M. S. P. *Proc. Natl. Acad. Sci. U.S.A.* **2003**, *100*(12), 7063–7068.
- (13) Yeh, I.-C.; Hummer, G. *Proc. Natl. Acad. Sci. U.S.A.* **2004**, *101*(33), 12177–12182.
- (14) Wang, J.; Zhu, Y.; Zhou, J.; Lu, X.-H. *Phys. Chem. Chem. Phys.* **2004**, *6*(4), 829–835.
- (15) Waghe, A.; Rasaiah, J. C.; Hummer, G. *J. Chem. Phys.* **2002**, *117*(23), 10789–10795.
- (16) Mann, D. J.; Halls, M. D. *Phys. Rev. Lett.* **2003**, *90*(19), 195503-1–195503-4.
- (17) Dellago, C.; Naor, M. M.; Hummer, G. *Phys. Rev. Lett.* **2003**, *90*(10), 105902.
- (18) Werder, T.; Walther, J. H.; Jaffe, R. L.; Halicioglu, T.; Koumoutsakos, P. *J. Phys. Chem. B* **2003**, *107*, 1345–1352.
- (19) Marković, N.; Andersson, P. U.; Någård, M. B.; Petterson, J. B. C. *Chem. Phys.* **1999**, *247*, 413–430.
- (20) Koumoutsakos, P.; Zimmerli, U.; Werder, T.; Walther, J. H. *The Handbook of Nanotechnology. Nanometer Structures. Theory, Modeling, and Simulation*; Lakhtakia, A., Ed.; SPIE/ASME, 2004, pp 319–393.
- (21) Berendsen, H. J. C.; Grigera, J. R.; Straatsma, T. P. *J. Phys. Chem.* **1987**, *91*, 6269–6271.
- (22) Essmann, U.; Perera, L.; Berkowitz, M. L.; Darden, T.; Lee, H.; Pedersen, L. G. *J. Chem. Phys.* **1995**, *103*(19), 8577–8593.
- (23) Vaitheeswaran, S.; Rasaiah, J. C.; Hummer, G. *J. Chem. Phys.* **2004**, *121*(16), 7955–7965.
- (24) Pohorille, A.; Wilson M. A. *Cell Mol. Biol. Lett.* **2001**, *6*, 369–372.
- (25) de Groot, B. L.; Grubmüller, H. *Science* **2001**, *294*, 2353–2357.

NL0503126